Bone 79 (2015) 150–161

Contents lists available at ScienceDirect

Bone

journal homepage: www.elsevier.com/locate/bone

Original Full Length Article

Overexpression of tissue-nonspecific alkaline phosphatase increases the expression of neurogenic differentiation markers in the human SH-SY5Y neuroblastoma cell line

Stephanie Graser [a], Birgit Mentrup [a], Doris Schneider [a], Ludger Klein-Hitpass [b], Franz Jakob [a,1], Christine Hofmann [c,*,1]

[a] Orthopedic Department, Orthopedic Center for Musculoskeletal Research, University of Wuerzburg, Germany
[b] Institute of Cell Biology, Faculty of Medicine, University of Duisburg-Essen, Germany
[c] Children's Hospital, Section of Pediatric Rheumatology and Osteology, University of Wuerzburg, Germany

ARTICLE INFO

Article history:
Received 22 January 2015
Revised 24 April 2015
Accepted 23 May 2015
Available online 29 May 2015

Edited by: Nuria Guanabens

Keywords:
Hypophosphatasia
Cellular processes
Overexpression
Transgenic
MAP2

ABSTRACT

Patients suffering from the rare hereditary disease hypophosphatasia (HPP), which is based on mutations in the *ALPL* gene, tend to develop central nervous system (CNS) related issues like epileptic seizures and neuropsychiatric illnesses such as anxiety and depression, in addition to well-known problems with the mineralization of bones and teeth. Analyses of the molecular role of tissue-nonspecific alkaline phosphatase (TNAP) in transgenic SH-SY5Y^{TNAPhigh} neuroblastoma cells compared to SH-SY5Y^{TNAPlow} cells indicate that the enzyme influences the expression levels of neuronal marker genes like RNA-binding protein, fox-1 homolog 3 (NEUN) and enolase 2, gamma neuronal (NSE) as well as microtubule-binding proteins like microtubule-associated protein 2 (MAP2) and microtubule-associated protein tau (TAU) during neurogenic differentiation. Fluorescence staining of SH-SY5Y^{TNAPhigh} cells reveals TNAP localization throughout the whole length of the developed projection network and even synapsin I co-localization with strong TNAP signals at some spots at least at the early time points of differentiation. Additional immunocytochemical staining shows higher MAP2 expression in SH-SY5Y^{TNAPhigh} cells and further a distinct up-regulation of tau and MAP2 in the course of neurogenic differentiation. Interestingly, transgenic SH-SY5Y^{TNAPhigh} cells are able to develop longer cellular processes compared to control cells after stimulation with *all-trans* retinoic acid (RA). Current therapies for HPP prioritize improvement of the bone phenotype. Unraveling the molecular role of TNAP in extraosseous tissues, like in the CNS, will help to improve treatment strategies for HPP patients. Taking this rare disease as a model may also help to dissect TNAP's role in neurodegenerative diseases and even improve future treatment of common pathologies.

Introduction

Hypophosphatasia is a rare multisystemic disease with enormous variations concerning age of clinical manifestation as well as variability and severity of symptoms. Molecular bases of HPP are various mutations in the *ALPL* gene (1p36.12, NCBI Gene-ID:249) which is coding for the ectoenzyme tissue-nonspecific alkaline phosphatase [1]. The predominant phenotype of this hereditary disease in its severe early onset manifestation is characterized by impaired bone mineralization and by disorganized growth plates with consecutive malformations [1]. Moreover, lung hypoplasia and functional impairment of the CNS , including epileptic seizures, may contribute to early death within weeks after birth [2]. Less severe forms of the disease with infantile, adolescent or even adult onset present with delayed bone mineralization, muscular problems like dynopenia, nephrocalcinosis, poor renal function or problems with the gastrointestinal tract [1]. Focusing on CNS-related issues, above all adult patients complain about sleep disturbances and neuropsychiatric

Abbreviations: 36B4, ribosomal protein, large, P0; AADC, aromatic L-amino acid decarboxylase; AD, Alzheimer's disease; ALPL/TNAP/Akp2, tissue-nonspecific alkaline phosphatase; AT, annealing temperature; ATP, adenosine triphosphate; ADP, adenosine diphosphate; AMP, adenosine monophosphate; BSA, bovine serum albumin; CNS, central nervous system; CNTNAP2, contactin associated protein-like 2; DCX, doublecortin; EEF1A, eukaryotic translation elongation factor 1 alpha 1; FBS, fetal bovine serum; GABA, gamma-aminobutyric acid; GAD, glutamate decarboxylase; GAPDH, glyceraldehyde-3-phosphate dehydrogenase; HPP, hypophosphatasia; MAP2, microtubule-associated protein 2; NEUN, RNA-binding protein, fox-1 homolog 3; NFASC, neurofascin; NPY, neuropeptide Y; NRP1, neuropilin 1; NRXN1, neurexin 1; NSE, enolase 2, gamma neuronal; P2X7, purinergic receptor P2X, ligand gated ion channel, 7; PBS, phosphate buffered saline; PGCs, primordial germ cells; PHOSPHO1, phosphatase, orphan 1; PI, protease inhibitor; PL, pyridoxal; PLP, pyridoxal 5′ phosphate; PRKCA, protein kinase c, alpha; RA, *all-trans* retinoic acid; RARβ, retinoic acid receptor β; RLU, relative light unit; ROBO2, roundabout, axon guidance receptor, homolog 2; SEM, standard error of mean; SEMA3A, semaphorin 3A; SVZ, subventricular zone; TAU, microtubule-associated protein tau.

* Corresponding author at: Children's Hospital, Section of Pediatric Rheumatology and Osteology, University of Wuerzburg, Josef-Schneider-Str. 2, 97080 Wuerzburg, Germany. Fax: +49 931 201627794.
E-mail address: hofmann_c5@ukw.de (C. Hofmann).

[1] F.J. and C.H. contributed equally to this work.

http://dx.doi.org/10.1016/j.bone.2015.05.033
8756-3282/

illnesses like increased nervousness, anxiety or depression (unpublished data of HPP patients' organization and our unpublished results). Such CNS-related symptoms in HPP underline the importance of TNAP enzyme in the neuronal system beyond its central and meanwhile quite well-understood role in bone metabolism.

Alkaline phosphatase is among others responsible for dephosphorylation of small molecule and polypeptide mineralization inhibitors such as inorganic pyrophosphate [3] and osteopontin [4] which finally balances and modulates the crystallization of hydroxyapatite [5]. As previously published by Narisawa et al. skeletal phenotypes in $Alpl^{-/-}$ mice (NCBI Gene-ID: 11647) can partly be attributed to accumulation of phosphorylated osteopontin [4]. Another key player in this system is the phosphatase PHOSPHO1 which supports the initiation of hydroxyapatite deposition in matrix vesicles whereas TNAP enables propagation of the newly formed crystals outside the vesicles [6,7]. As a consequence, combined ablation of PHOSPHO1 and TNAP completely prevents skeletal mineralization [7]. In addition, adenosine triphosphate (ATP), diphosphate (ADP) and monophosphate (AMP) are further substrates for TNAP [8,9] thus contributing to changes in the microenvironmental concentrations of purine-derived compounds that orchestrate purinergic signaling via a series of receptors and ligand-modulated channels as well as adenosine receptors. Purinergic signaling is relevant in several tissues including bone and the central nervous system [10].

No brain-specific transcripts of TNAP have been found so far as all analyzed neuronal and endothelial cells in humans, marmosets and rats solely express the bone specific *ALPL* transcript, whereas mouse neurons also express liver transcripts [11]. Moreover, expression of tissue-nonspecific alkaline phosphatase changes in accordance with the developmental stage of the brain [11]. In the human neocortex TNAP expression can be found in layer 5 throughout the frontal-, temporal- and occipital lobes [12]. Further, alkaline phosphatase activity is localized in the neuropile alongside the thalamo-cortical innervations in layer 4 of primary visual, auditory and somatosensory cortices and furthermore varies depending on sensory experience. Subcellular localization of TNAP enzyme is characterized by accumulation at synaptic junctions during maturation, its distribution matches GAD_{65} localization at presynaptic terminals and apart from that alkaline phosphatase is distributed alongside the axon solely in myelin-free parts [13,14]. Consistent with those results Hanics et al. published that TNAP knockout mice ($Akp2^{-/-}$) display severe dysfunctions as far as central processes like myelination and maturation of synapses are concerned [15]. Moreover, TNAP enzyme might influence migration of primordial germ cells (PGCs) and neurons due to its ability of interaction with extracellular matrix proteins like collagen and further regulates proliferation and differentiation of neural stem cells into neurons or oligodendrocytes [16,17]. Experiments with murine neurons isolated from hippocampus samples revealed a connection between TNAP and axonal growth. TNAP staining shows prominent signals in somatic and axonal regions. The strongest signals are located at axon terminals and branching points, whereas only weak signals could be detected in dendrites [18]. TNAP inhibition impairs axonal growth significantly, probably due to elevated ATP levels that activate P2X7 receptors at the growth cone, which prevents axonal growth. In contrast, no effects of TNAP inhibition could be seen on dendritic outgrowth [18]. Moreover, TNAP might influence neurogenesis during mouse brain development and expression was found in the subventricular zone in adult mouse brains, which is one of the few regions where adult neurogenesis takes place [19]. Above all, TNAP is crucial for vitamin B_6 metabolism as only the transport form pyridoxal (PL) is able to cross the blood–brain barrier and functional TNAP is indispensable for dephosphorylation of pyridoxal-5′-phosphate (PLP). PL is activated through rephosphorylation after passing the blood–brain-barrier and serves as a cofactor for enzymes playing a central role in neurotransmitter metabolism, like aromatic L-amino acid decarboxylase (AADC) and glutamate decarboxylase (GAD) which regulate synthesis of serotonin, dopamine, (nor-)/adrenalin and GABA [20–22]. A recent publication describes quite conserved TNAP localization in the retina across many species and therefore suggests a potential role for retinal neurotransmission [23].

In order to reveal further details about the molecular function of TNAP in neuronal systems we established a neuroblastoma cell line which stably over-expresses TNAP enzyme (SH-SY5Y^{TNAPhigh}) and compared its gene expression patterns and morphology with and without treatment with neurogenic differentiation media to parent cells (SH-SY5Y^{TNAPlow}). Using this human *in vitro* model turned out to be a very promising tool in order to confirm and extend knowledge on the role of alkaline phosphatase concerning neurogenic differentiation and maturation. Literature gives information about localization of TNAP in mouse brains [17,24] and about the enzyme's role during axonal growth in murine hippocampal neurons [18] as well as during differentiation of murine neural stem cells [16]. Information about the distribution in the human neocortex was gained from histological analysis [12,13]. Using our in vitro model, we are able to further dissect the role of TNAP on consecutive events during differentiation and maturation in neuronal cell lines of human origin.

We can demonstrate here that TNAP overexpression profoundly influences outgrowth of cellular processes and expression of neuronal differentiation markers during neuronal cell differentiation, indicating that TNAP is capable of modulating intercellular communication in the CNS. Interestingly only certain cells in layer 4 and layer 5 of the human neocortex are TNAP positive whereas surrounding cells are not [12,13]. Our established *in vitro* model enables us to analyze possible roles of those cells in human context and provides additional knowledge to previously published literature data gained in mouse models.

Materials and methods

Cell culture

Neuroblastoma cell line SH-SY5Y (ATCC:CRL-2266) was kindly provided by Prof. Lesch (Department of Psychiatry, Psychosomatics and Psychotherapy, University of Wuerzburg, Germany) and cultured in DMEM Ham's F12 media (Life Technologies GmbH, Darmstadt, Germany) supplemented with 10% heat inactivated FBS (Biochrom AG, Berlin, Germany), 100 nM sodium selenite and 50 μg/ml gentamicin (both Sigma-Aldrich, Munich, Germany). Cells grew constantly at 37 °C and 5% CO_2 and were negatively tested for mycoplasma contamination by DAPI staining.

Plasmids and transfection

SH-SY5Y^{TNAPlow} cells were transfected using the reagent Lipofectamin 2000 according to manufacturer's instructions (Invitrogen GmbH, Darmstadt, Germany) with a SSP1 (New England Biolabs GmbH, Frankfurt/Main, Germany) linearized pcDNA3.1-vector (Invitrogen GmbH, Darmstadt, Germany) containing the coding region of the human *ALPL* gene in order to establish the cell line SH-SY5Y^{TNAPhigh}. The overexpression construct was previously described in literature [25]. A second cell line, SH-SY5Y$^{pcDNA3.1}$, containing the empty vector, was established equivalently for control purposes. Both stable cell lines were cultured in media containing 300 μg/ml G418 (BD Biosciences Clontech, Heidelberg, Germany) for selection of cells containing the respective constructs.

Isolation of RNA

Total RNA was isolated with the Nucleo Spin RNA II Kit (Macherey-Nagel GmbH and Co. KG, Düren, Germany) according to manufacturer's instructions.

Semi-quantitative PCR (RT-PCR)

For RT-PCR analysis 1 μg of total-RNA was reversely transcribed with the enzyme MMLV reverse transcriptase using oligo-dT_{12-18}-Primer (both Promega GmbH, Mannheim, Germany) in a total volume of 25 μl. For semi-quantitative PCR 5 μl 10× reaction buffer S, 0.2 mM dNTPs each, 2.5 mM $MgCl_2$ (incl. 1.5 mM in reaction buffer S), 0.02 unit/μl Taq-DNA-polymerase (all purchased from Peqlab Biotechnologie GmbH, Erlangen, Germany), 0.1 μM sense and antisense primer (Eurofins MWG GmbH, Ebersberg, Germany), 1– μl cDNA was used and filled up to a total volume of 50 μl with RNase-free H_2O (Carl Roth GmbH & Co. KG, Karlsruhe, Germany). The respective amount of H_2O was added instead of cDNA as negative control. PCR conditions were as follows: 94 °C 3 min; 72 °C 2 min; [94 °C 30 s; primer specific annealing temperature (AT) 30 s; 72 °C 40 s] repeated 21–45 times; AT 30 s; 72 °C 2 min; 10 °C 10 min. The following primer combinations (listed in 5′–3′ direction) were used: **EEF1A_s**: CTGTATTGGA TTGCCACACG + **EEF1A_as**: AGACCGTTCTTCCACCACTG 55 °C 21 cycles; **ALPL_s**: GCTGAACAGGAACAACGTGA + **ALPL_as**: AGAC TGCGCCTGGTA GTTGT 57 °C 40 cycles; Oligonucleotides were designed with the software Primer3Web Version 3.0.0. Product size was analyzed by agarose gel electrophoresis using a 100 bp marker (Peqlab Biotechnologie GmbH, Erlangen, Germany) as size control.

Quantitative real-time PCR (qPCR)

For qPCR analysis 0.54 to 1.0 μg RNA was reversely transcribed into cDNA which was diluted 1:5 in H_2O afterwards. qPCRs were performed in a total volume of 20 μl by using 10 μl KAPA SYBR Fast Universal mix for qPCR (Peqlab Biotechnologie GmbH, Erlangen, Germany), 0.25 μM of each sense and antisense primer (Eurofins MWG GmbH, Ebersberg, Germany) and 1 μl of cDNA. Reaction mix was filled up to 20 μl with RNase free H_2O. For MAP2 as well as for TAU PCRs only 0.125 μM of each primer were used and for NEUN-PCR 5 μl cDNA, instead of 1 μl, were used per sample. Following primer combinations (listed in 5′–3′ direction) were used with the stated conditions (Table 1).

RPS27A and 36B4 were used as housekeeping genes. Oligonucleotides for MAP2 were used as published by Joo-Hee Lee et al. [26] and the remaining oligonucleotides were designed with the software Primer3Web Version 3.0.0. The following program was used for running the qPCRs in Opticon DNA engine (MJ Research, Waltham, USA): 3 min 95 °C, [5 s 95 °C; 15 s AT, 5 s 72 °C] repeated 40 times followed by a melting curve from 45 °C–95 °C for analysis of product specificity. Results were statistically evaluated with the software REST 2009V2.0.13 (QIAGEN GmbH, Hilden, Germany) [27]. Experiments as well as qPCRs were performed three times independently in order to guarantee reliable results.

Neurogenic differentiation

In order to differentiate the three different neuroblastoma cell lines 4.0×10^3 cells/cm^2 were seeded on collagen coated ground (rat tail collagen I, Corning B.V., Amsterdam, NL) and neurogenic differentiation media was modified on the basis of a previously published work [28]. DMEM Ham's F12 with L-glutamine was supplemented with 0.1% FBS (Biochrom AG, Berlin, Germany), 100 nM sodium selenite, 50 μg/ml gentamicin, 1 μM *all-trans* retinoic acid, 0.9 μM insulin, 20 nM progesterone, 100 μg/ml apo-transferrin and 100 μM putrescine (all purchased from Sigma Aldrich, Munich, Germany). Medium was changed after 3–4 days.

Measurement of cellular processes

Morphological analysis was conducted with the microscope AxioVert 25 (Carl Zeiss Microscopy GmbH, Jena, Germany) and the software Axio Vision Rel. 4.8. Differentiation experiments were carried out three times independently. Eight pictures of each cell line were taken in each experiment at the starting point (t_0) and after 1, 4, 6 and 8 days of cultivation with differentiation media (20× magnification). Lengths of 10 cellular processes per randomly coded photo were measured with the software ImageJ 1.49j. The lengths were measured from the cell body until the end, always choosing the longest distance. The number of branching points was not considered separately. Mean values and SEM were calculated of a total of 240 (at least 140) values per cell line per time point. For statistics a two-way ANOVA with Tukey post-hoc test was calculated with IBM SPSS Statistics 22. p-values < 0.05 were considered as significant.

RNA analysis during neurogenic differentiation

For comparative gene expression analysis cells were seeded in a density of 4.0×10^3 cells/cm^2 and differentiated according to the protocol described above. Cells were harvested at t_0, day 1, day 3, day 6 and day 10 for qPCR analysis (details see Isolation of RNA and Quantitative real-time PCR (qPCR).

Table 1
Used primer combinations for qPCRs stated in 5′–3′ direction with specific annealing temperature (AT). 36B4 (ribosomal protein, large, P0), CNTNAP2 (contactin associated protein-like 2), DCX (doublecortin), MAP2 (microtubule-associated protein, 2), NEUN (RNA-binding protein, fox-1 homolog 3), NFASC (neurofascin), NPY (neuropeptide Y), NRP1 (neuropilin 1), NRXN1 (neurexin 1), NSE (enolase 2, gamma neuronal), PRKCA (protein kinase c, alpha), RARβ (retinoic acid receptor, beta), ROBO2 (roundabout, axon guidance receptor, homolog 2), RPS27A (ribosomal protein S27a), SEMA3A (semaphorin 3A) and TAU (microtubule-associated protein tau).

Gene name	AT (+T of melting step)	Sense	Antisense
36B4	60 °C	TGCATCAGTACCCCATTCTATCAT	AGGCAGATGGATCAGCCAAGA
CNTNAP2	59 °C	GGATGCTCTACAGCGACACA	TCTCCATTCCAATCCAGAGG
DCX	61 °C	GCCGAGTCATGAAGGGAAAC	GAGGTTCCGTTTGCTGAGTC
MAP2	60 °C	CATGGGTCACAGGGCACCTATTC	GGTGGAGAAGGAGGCAGATTAGCTG
NEUN	61 °C	CTTACGGAGCGGTCGTGTAT	TCACATGGTTCCAATGCTGT
NFASC	61 °C (+83 °C)	TCCTGGGCAAAGCTGAAAAC	AGACGGTGAGTTTCAGGGAG
NPY	60 °C	GCTGCGACACTACATCAACC	CACCACATTGCAGGGTCTTC
NRP1	59 °C	GAAGCACCGAGAGAACAAGG	GTTGCCCTCAAAAGACTTCG
NRXN1	61 °C	AGGACATTGACCCCTGTGAG	GGCTACTATCCCAACGACCA
NSE	60 °C	CCCAGAACTTCCCTGATTGA	AAGTGGAAGACACGTGGGAC
PRKCA	61 °C	TATCGCCCCAGAGATAATCG	CCTTGGACAAGGATTTTGGA
RARβ	61 °C	GGTTTCACTGGCTTGACCAT	AAGGCCGTCTGAGAAAGTCA
ROBO2	60 °C	CCAAGGAGATCCTCAACCAA	TTTTCCAACCCGATTCTCAG
RPS27A	60 °C	TCGTGGTGGTGCTAAGAAAA	TCTCGACGAAGGCGACTAAT
SEMA3A	61 °C	TGGACATCATCCTGAGGACA	CAAAGTCTCGCCCCATAAAA
TAU	60 °C	AAGGTGACCTCCAAGTGTGG	TATTGTCCAGGGACCCAATC

Table 2
Primary and secondary antibodies for immunostaining.

Antibody	Host	Supplier	Dilution
MAP2 (M3696)	Rabbit	Sigma-Aldrich, Munich, Germany	1:200
MAP2 (MAB3418)	Mouse	Millipore S.A.S, Molsheim, France	1:250
Synapsin I (ab8)	Rabbit	Abcam, plc, Cambridge, UK	1:500
Tau (H-150) sc-5587	Rabbit	Santa Cruz Biotechnologie, Heidelberg, Germany	1:100
TNAP (B4-78) sc-81754	Mouse	Santa Cruz Biotechnologie, Heidelberg, Germany	1:200
Anti-rabbit NL557	Donkey	R + D Systems GmbH, Wiesbaden-Nordenstadt, Germany	1:400
Anti-mouse NL009	Donkey	R + D Systems GmbH, Wiesbaden-Nordenstadt, Germany	1:400
Anti-mouse NL557	Donkey	R + D Systems GmbH, Wiesbaden-Nordenstadt, Germany	1:400

Immunocytochemistry

For comparison of TNAP expression 3.0×10^5 cells were seeded on cover slips in a 6-well plate and grew approximately 24 h. For staining of differentiating cells 4.0×10^3 cells/cm^2 of the respective cell line were seeded on sterile and collagen I coated cover slips in 6-well plates and treated with differentiation media for 72 h or 0, 1, 4, 6, and 8 days respectively. Cells were then washed with PBS once and fixed with ice-cold methanol/acetone (1:1) for 5 min. After 10 minute drying cells were stored at −80 °C. Before staining, the cells were washed with PBS 3× 5 min and treated with 0.05% PBS-Tween20 for 15 min in order to increase permeability of cell membranes. After 2× 5 min washing steps a 3% BSA/PBS solution was applied 30 min for blocking purposes. Then samples were washed with PBS (3× 5 min) and the primary antibodies were diluted in 1% BSA/PBS (see Table 2). Equally concentrated mouse or rabbit serum (Santa Cruz Biotechnologie, Heidelberg, Germany) were used as controls instead of the primary antibodies in order to exclude reactivity with unspecific mouse or rabbit antigens. After incubation with the primary antibody (4 °C, over night) cells were washed with PBS 3× 5 min and treated with the secondary antibody, which was diluted in 1% BSA/PBS (see Table 2), 1.5 h at room temperature. Samples were covered with Vectashield H-1200 + DAPI after another three washing steps (Linaris Biologische Produkte GmbH, Dossenheim, Germany) and analyzed at the fluorescence microscope Axioskop 2 (Carl Zeiss Jena, Jena, Germany) using the software AxioVision Rel 4.8.

CSPD-assay: measurement of alkaline phosphatase activity

In order to measure the enzymatic activity of alkaline phosphatase in SH-SY5Y^{TNAPlow}, SH-SY5Y$^{pcDNA3.1}$ and SH-SY5Y^{TNAPhigh} cells, they were seeded in a density of 1.0×10^6 in 25 cm^2 cell culture flasks and cultivated until they reached 80–90% confluence. Cells were harvested in 200 μl PBS supplemented with protease inhibitor complete (PI) (Roche GmbH, Mannheim, Germany) 25:1 on ice, sonified on ice and centrifuged 10 min at 10,000 rpm and 4 °C. Afterwards, protein content was measured with RotiQuant (Carl Roth GmbH & Co. KG, Karlsruhe, Germany) using a BSA dilution series as reference. Samples were diluted to a total protein concentration of 0.01 μg/μl using PBS/PI (with or without 10 mM of the TNAP specific inhibitor levamisole, Sigma-Aldrich, Munich, Germany). 100 μl of each sample was pipetted into a 96-well plate in technical triplicates. 100 μl of CSPD ready-to-use reagent (0.25 mM solution; Roche GmbH, Mannheim, Germany) was added (final concentration of 5 mM levamisole) and luminescence signals were measured at an Orion II Microplate Luminometer (Berthold Detection Systems, Pforzheim, Germany) after an incubation time of 5 min at 37 °C. CSPD-assay was modified based on a publication by Ermonval et al. [29]. Data were calculated as means of technical triplicates gained from three experiments and the SEM is shown. For statistical analysis two-tailed Mann–Whitney-U test was calculated either in reference to SH-SY5Y^{TNAPlow} without levamisole or as comparison of values for one cell line +/− levamisole. Values with $p < 0.05$ were considered as significantly different.

Western blot

5.0×10^6 cells were seeded in 75 cm^2 flasks, cultivated until 80–90% confluence was reached and harvested in 350 μl RIPA-buffer (Sigma-Aldrich, Munich, Germany) + PI (25:1) on ice and stored at −20 °C. Cells were then sonified on ice and centrifuged 10 min at 10,000 rpm (4 °C) in order to generate whole cell lysates. Protein content was measured with RotiQuant (Carl Roth GmbH & Co. KG, Karlsruhe, Germany) using a BSA dilution series as reference. Lysates were diluted to a total of 15 μg protein content in 12 μl RIPA/PI and 4 μl RotiLoad (Carl Roth GmbH & Co. KG, Karlsruhe, Germany) was added. Samples were boiled in a water bath for 5 min and immediately stored on ice. Separation took place on a polyacrylamide gel (MDE solution obtained from Biozym Scientific GmbH, Hessisch Oldendorf, Germany) under denaturing conditions using protein marker V (Peqlab Biotechnologie GmbH, Erlangen, Germany) as a reference for size. Samples were blotted onto a nitrocellulose membrane Optitran BA-S85 (GE Healthcare Europe GmbH, Freiburg, Germany) for 2 h (20 V), using a Mini protean unit (BioRad München, Germany) placed on ice and pre-cooled transfer buffer containing 10% 0.25 M Tris/1.9 M Glycin (pH 10) and 20% methanol in H_2O. After the blotting procedure, the membrane was incubated with a blocking solution containing 2.5% BSA, 2.5% non-fat milk powder (both AppliChem GmbH, Darmstadt, Germany) and 2% horse serum (Biochrom AG, Berlin, Germany) in 0.1% PBS-Tween20 for 2 h. Incubation with the primary antibody TNAP (B4-78) sc-81754 (Santa Cruz Biotechnology, Heidelberg, Germany), diluted 1:400 in incubation solution containing 1% BSA, 1% not-fat milk powder and 1% horse serum in PBS-0.1% Tween-20, was done overnight at 4 °C. GAPDH sc-137179 (Santa Cruz Biotechnology, Heidelberg, Germany) was used in a 1:1000 dilution respectively as a loading control. Membrane was washed 3× 10 min with 1% BSA, 1% not-fat milk powder and 1% horse-serum in a solution containing 10 mM Tris–HCl (pH 7.5), 150 mM NaCl, 2 mM EDTA (pH 8.0) and 0.1% Triton X-100. After 2 h incubation with the secondary antibody goat anti-mouse IgG-HRP sc-2005 (Santa Cruz Biotechnology, Heidelberg, Germany) which was diluted 1:2000 in incubation solution, 3× 10 min washing procedure with 1% BSA, 1% not-fat milk powder and 1% horse-serum in a solution containing 10 mM Tris–HCl (pH 7.5), 1 M NaCl, 2 mM EDTA (pH 8.0) and 0.1% Triton X-100 followed. Membrane was incubated with ECL solution (GE Healthcare Europe GmbH, Freiburg, Germany) for 1.5 min and chemiluminescence signals were detected by film exposure (VWR International GmbH, Darmstadt, Germany).

Microarray and GOstat analysis

GOstat analysis was executed after microarray hybridization in order to find overrepresented gene ontologies within the group of up-regulated genes [30]. GOstat analysis was performed after comparative hybridizations of SH-SY5Y^{TNAPlow} and SH-SY5Y^{TNAPhigh} RNA on an Affymetrix GeneChip HGU133 Plus 2.0 in technical triplicates. Hybridization was done by PD Dr. Klein-Hitpass (Institute of Cell Biology, Faculty of Medicine, University of Duisburg-Essen, Germany). GOstat analysis of up-regulated genes was done on http://bioinfo.vanderbilt.

edu/webgestalt/ with a logarithmic fold-change ≥ 1 as inclusion criteria. Furthermore, each group had to contain at least five different genes and results were considered as significant if p-value < 0.05.

Results

Characterization of SH-SY5Y^{TNAPhigh} cell line proves elevated TNAP expression on RNA and protein levels as well as increased enzymatic activity

The stable integration of the linearized pcDNA3.1_TNAP and pcDNA3.1 sequence (empty control vector) respectively into the genome of SH-SY5Y^{TNAPlow} cells is confirmed by semi-quantitative PCRs with a combination of vector-specific and TNAP-specific primer pairs and genomic DNA as a template (data not shown). Analysis of mRNA reveals significantly higher expression of TNAP in SH-SY5Y^{TNAPhigh} compared to SH-SY5Y^{TNAPlow} and the cell line, which has integrated the empty vector alone (SH-SY5Y$^{pcDNA3.1}$) as second control (Fig. 1A). Amplification of EEF1A as a reference gene shows equal expression in all three approaches.

Furthermore, TNAP protein expression was analyzed by Western blotting with specific antibodies. The signal at approximately 80 kDa resembles the functional, post-translationally modified protein and is very prominent in the SH-SY5Y^{TNAPhigh} cell line, whereas no detectable signal can be seen in SH-SY5Y^{TNAPlow} and SH-SY5Y$^{pcDNA3.1}$. GAPDH was used as loading control and shows a similar expression in all three cell lines (Fig. 1B). The activity of the enzyme was tested in a CSPD-assay. It is over 1000-fold elevated in SH-SY5Y^{TNAPhigh} whole cell lysates compared to SH-SY5Y^{TNAPlow} ($p < 0.001$) and SH-SY5Y$^{pcDNA3.1}$ which proves the biological functionality of the overexpressed protein and the very low TNAP levels in the control cells. As values around 25–30 RLUs can be considered as background, no difference after levamisole treatment in SH-SY5Y^{TNAPlow} and SH-SY5Y$^{pcDNA3.1}$ can be detected. 5 mM of the TNAP-specific inhibitor levamisole are able to minimize the signal approximately 0.02-fold ($p < 0.001$) in SH-SY5Y^{TNAPhigh} cells (Fig. 1C). Consistent with the Western blot results and the functional activity, the positive fluorescence signal in SH-SY5Y^{TNAPhigh} clarifies the expected localization of TNAP in the cell membrane. Neither SH-SY5Y^{TNAPlow}, SH-SY5Y$^{pcDNA3.1}$ nor the negative control, which was treated with mouse serum instead of the primary antibody (white box), shows green fluorescence signals (Fig. 1D).

GOstat analysis shows correlations between TNAP expression and neurogenic differentiation

In order to analyze differences in gene expression under the influence of strong TNAP overexpression, a microarray analysis was performed. 635 probesets are down-regulated (log fold change ≤ −1) and 512 probesets are up-regulated (log fold change ≥ 1) in SH-SY5Y^{TNAPhigh} samples compared to SH-SY5Y^{TNAPlow}. Furthermore, GOstat analysis of up-regulated genes reveals an over-representation of gene groups containing above all relevant genes for neurogenesis, axon growth and neuron development (Table 3).

Genes of interest were selected for biological validation of *in silico* data, based on the results of GOstat analysis and the respective fold changes, and subsequently analyzed via qPCR, using five biological replicates of each cell line. The expression of the neuronal marker NEUN was analyzed independently from the microarray analysis.

The differentially expressed genes are listed in Table 4. SH-SY5Y^{TNAPhigh} cells show a significant down-regulation of ROBO2, NRP1 and its ligand SEMA3A, whereas CNTNAP2, NRXN1, DCX, PRKCA and NEUN are up-regulated in comparison to the cells with low endogenous TNAP level (Table 4). The downregulation of ROBO2 is nonetheless inconsistent with the microarray data, which suggest an upregulation in SH-SY5Y^{TNAPhigh} cells.

A second GOstat analysis based on another microarray analysis with SH-SY5Y^{TNAPlow} and SH-SY5Y^{TNAPhigh} cells that have been treated with neurogenic differentiation media for 72 h ($n = 1$) reveals very similar gene ontologies and further increases confidence in the reported results (data not shown).

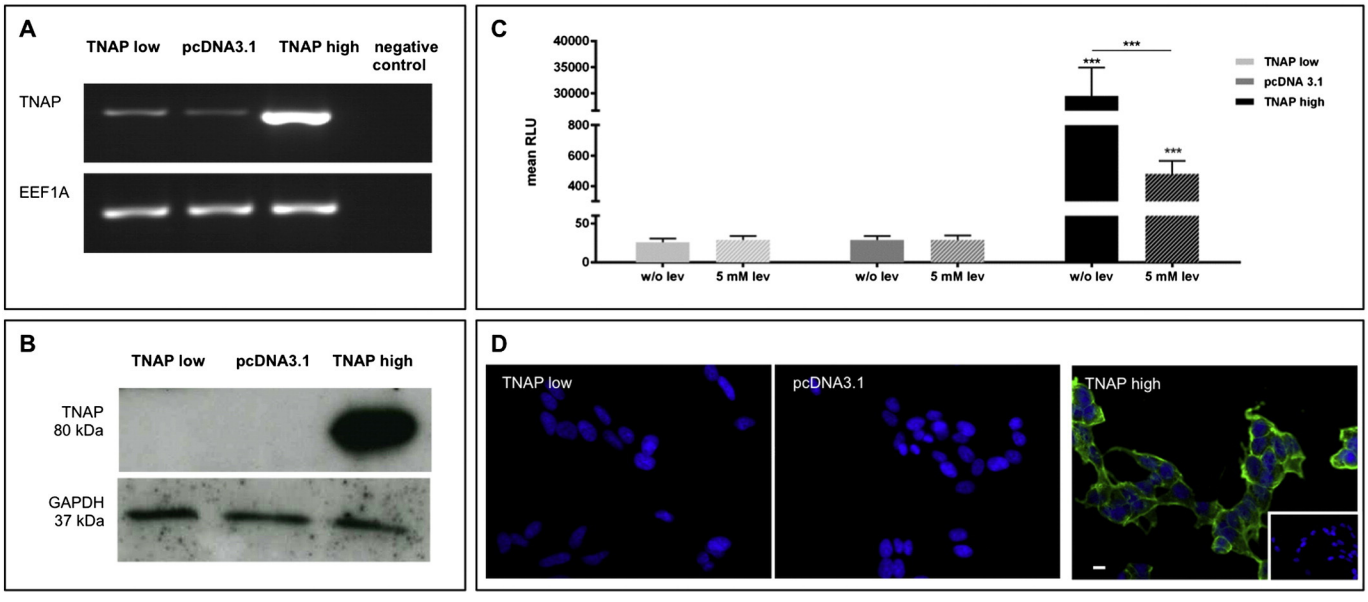

Fig. 1. A. RT-PCR shows a significantly higher expression of TNAP in SH-SY5Y^{TNAPhigh} compared to the other two cell lines. The housekeeping gene EEF1A was used for normalization. B. Western blot analysis with TNAP-specific antibody shows no signal in SH-SY5Y^{TNAPlow} and SH-SY5Y$^{pcDNA3.1}$ cell lysates, but a very strong band at approx. 80 kDa in SH-SY5Y^{TNAPhigh} cells which resembles the TNAP protein. GAPDH (37 kDa) was used as reference protein and 15 μg of protein lysate were loaded per lane. C. SH-SY5Y^{TNAPhigh} cell lysates (black bar) show highly elevated enzymatic activity of alkaline phosphatase in CSPD-assays which can be reduced dramatically by addition of 5 mM TNAP-specific inhibitor levamisole (shaded bars). Independent experiments were carried out three times with technical triplicates each. Mean of relative light units (RLUs) of 9 values and SEM is depicted. For statistical analysis two-tailed Mann–Whitney-U test was calculated. ***$p < 0.001$. D. Immunocytochemical staining of TNAP (green) shows localization of the enzyme in the plasma membrane of SH-SY5Y-^{TNAPhigh}, whereas no signals could be detected in the other two cell lines. DAPI staining (blue) was used for visualization of the nuclei. Reactivity with unspecific mouse antigens was excluded, since no staining could be seen in samples, which were treated with mouse serum instead of the primary antibody (white box). Pictures were taken at 40× magnification and scale bar represents 10 μm. (For interpretation of the references to color in this figure legend, the reader is referred to the web version of this article.)

Table 3
Results of GOstat analysis comparing expression of SH-SY5Y^{TNAPhigh} and SH-SY5Y^{TNAPlow} point out a positive influence of TNAP on neuron differentiation and projection development. Up-regulated genes in SH-SY5Y^{TNAPhigh} compared to SH-SY5Y^{TNAPlow} (fold change ≥ 1) are subdivided into different GO groups.

Biological process----neuron differentiation----GO:0030182
ALCAM; CAMK2B; CBFA2T2; CNTN1; CNTNAP2; CSNK2A2; EGFR; FRZB; GAS7; GATA3; GPC2; HOXD3; LAMB1; LEF1; LIFR; MYO16; NRCAM; NRXN1; NTM; PMP22; PRKCA; PRKD1; PTPRO; PTPRR; ROBO2; S100A6; S100B; SEMA6A; SPAG9; TCF4; UBE4B; UNC5A.
Biological process----generation of neurons----GO:0048699
ALCAM; CAMK2B; CBFA2T2; CNTN1; CNTNAP2; CSNK2A2; EGFR; FRZB; GAS7; GATA3; GPC2; HOXD3; LAMB1; LEF1; LIFR; MYCN; MYO16; NF1; NRCAM; NRXN1; NTM; PMP22; PRKCA; PRKD1; PTPRO; PTPRR; ROBO2; S100A6; S100B; SEMA6A; SPAG9; TCF4; UBE4B; UNC5A.
Biological process----neuron projection development----GO:0031175
ALCAM; CAMK2B; CBFA2T2; CNTN1; CNTNAP2; CSNK2A2; EGFR; FRZB; GAS7; GATA3; LAMB1; LIFR; MYO16; NRCAM; NRXN1; NTM; PMP22; PRKCA; PRKD1; PTPRO; ROBO2; S100A6; S100B; SEMA6A; UBE4B; UNC5A.
Biological process----neurogenesis----GO:0022008
ALCAM; CAMK2B; CBFA2T2; CNTN1; CNTNAP2; CSNK2A2; EGFR; FRZB; GAS7; GATA3; GPC2; HOXD3; LAMB1; LEF1; LIFR; MYCN; MYO16; NF1; NRCAM; NRXN1; NTM; PMP22; PRKCA; PRKD1; PTPRO; PTPRR; ROBO2; S100A6; S100B; SEMA6A; SPAG9; TCF4; UBE4B; UNC5A.
Biological process----neuron development----GO:0048666
ALCAM; CAMK2B; CBFA2T2; CNTN1; CNTNAP2; CSNK2A2; EGFR; FRZB; GAS7; GATA3; LAMB1; LIFR; MYO16; NRCAM; NRXN1; NTM; PMP22; PRKCA; PRKD1; PTPRO; ROBO2; S100A6; S100B; SEMA6A; UBE4B; UNC5A.
Cellular component----axon----GO:0030424
AAK1; ALCAM; CADM2; CNTNAP2; DDC; GRIA3; NF1; NRCAM; NRXN1; NTM; PTPRN2; PTPRO; ROBO2; SEMA6A; SEPT6;
Cellular component----anchored to membrane----GO:0031225
ALPL; CNTN1; FOLR1; GGTA1P; GPC2; GPC3; LSAMP; NTM.
Cellular component----axon part----GO:0033267
AAK1; CNTNAP2; GRIA3; NRCAM; NRXN1; PTPRN2; ROBO2; SEPT6.

Based on the results of the microarray analysis and of subsequently performed experiments, we decided to examine TNAP's impact on the process of neurogenic differentiation more closely. We therefore performed fluorescence staining, qPCRs and morphological analyses.

TNAP is localized throughout the whole cellular processes and co-localized with synapsin I at some spots

At first immunocytochemical staining with specific antibodies against TNAP ectoenzyme was carried out in order to visualize its localization in growing processes during neurogenic differentiation of SH-SY5Y^{TNAPhigh} cells. Fig. 2A shows that TNAP (green) is located at the membrane of the cell bodies as well as throughout the whole cellular projection network. Moreover, some cells show clustered TNAP staining at specific spots of the processes. In order to analyze, whether those spots are branching points or developing synapses, we performed double-staining of TNAP and synapsin I (Figs. 2B–E). Those experiments reveal strong signals for the synaptic marker synapsin I and TNAP at some tips of the cellular processes, respectively at spots where two processes get in touch with each other after 72 h of treatment. Nonetheless, only some cells show this phenomenon and by far not all. Additional analysis of synapsin I expression at day 8 of neurogenic differentiation reveals a clear increase of positive signals within the network compared to day 3, but no clear correlation between strong TNAP and synapsin I signals could be seen (data not shown). Cells treated with mouse and rabbit serum (white box) do neither show green nor red fluorescence signals, excluding reactivity of the secondary antibodies with unspecific mouse or rabbit antigens.

Table 4
Analysis of the relative gene expression in SH-SY5Y^{TNAPhigh} compared to SH-SY5Y^{TNAPlow} cells via qPCR confirms differentially expressed genes. ROBO2 (roundabout, axon guidance receptor, homolog 2), NRP1 (neuropilin 1) and SEMA3A (semaphorin 3A) are significantly down-regulated whereas CNTNAP2 (contactin associated protein-like 2), NRXN1 (neurexin 1), DCX (doublecortin), PRKCA (protein kinase c, alpha) and NEUN (RNA binding protein, fox-1 homolog (*C. elegans*) 3) are significantly up-regulated in SH-SY5Y^{TNAPhigh} compared to SH-SY5Y^{TNAPlow} cells. Five biological replicates of each cell line were analyzed, qPCR was pipetted three times and 36B4 (ribosomal protein, large, P0) and RPS27A (ribosomal protein S27a) were used as reference genes for normalization.

Gene name	Fold change TNAP high/TNAP low	Standard error	p-value
ROBO2	0.439	0.107–2.801	0.004
NRP1	0.295	0.121–0.579	<0.001
SEMA3A	0.188	0.031–0.923	0.001
CNTNAP2	1.711	0.520–6.123	0.005
NRXN1	1.808	0.863–3.777	0.003
DCX	2.629	1.112–5.996	<0.001
PRKCA	4.296	2.208–8.827	<0.001
NEUN	5.759	0.890–31.289	0.001

Typical neuronal markers show higher expression levels in SH-SY5Y^{TNAPhigh} than in SH-SY5Y^{TNAPlow} cells in the course of neurogenic differentiation

In order to prove whether RA stimulation causes a response within the cells, the expression of the receptor RARβ, which is known to be up-regulated by RA stimulation [31], was analyzed. The relative expression changes of RARß in SH-SY5Y^{TNAPlow} is 6.879 fold ($p = 0.010$) after treatment with RA (1 day) compared to t_0, which shows a robust and significant up-regulation of the RARβ gene after treatment. Interestingly, SH-SY5Y^{TNAPhigh} cells show a fold change of 17.845 comparing stimulated cells at day 1 to untreated ones at t_0 ($p = 0.003$).

Additionally performed RT-PCRs with SH-SY5Y^{TNAPlow} cells show an increase of TNAP expression after treatment with RA (Suppl. Fig. 1). Consequently, the stimulation with RA induces changes in specific gene expression patterns. As SH-SY5Y^{TNAPhigh} cells show a stronger response to stimulation with RA, consistent with a higher susceptibility to neurogenic commitment, we wanted to examine whether typical neuronal markers like MAP2 and NEUN are also up-regulated in a stronger manner. Analysis of marker genes by qPCR indicates that NEUN, TAU, NPY and NSE show a higher expression level in TNAP overexpressing cells from day 1 until day 10. NEUN and NPY increase their expression only in SH-SY5Y^{TNAPhigh} cells, whereas TAU and NSE show a prominent rise in both cell lines. MAP2 and NFASC interestingly show a higher expression level in SH-SY5Y^{TNAPhigh} cells between day 1 and day 6, but SH-SY5Y^{TNAPlow} show a sudden increase resulting in a higher expression of those genes compared to TNAP positive cells at day 10 (Fig. 3). We also analyzed the expression of the typical stem cell marker nestin, but did not see any significant decrease neither in SH-SY5Y^{TNAPlow} nor in SH-SY5Y^{TNAPhigh} cells during our experimental setup (data not shown). PRKCA expression stays on a high level in SH-SY5Y^{TNAPhigh} compared to SH-SY5Y^{TNAPlow} cells and shows just slight changes in expression levels during treatment with differentiation medium. SH-SY5Y^{TNAPlow} cells show a significant decrease in PRKCA expression at day 6. NRP1 expression rather stays on a significantly lower level in SH-SY5Y^{TNAPhigh} cells compared to SH-SY5Y^{TNAPlow} day 1 whereas those cells show a slight decrease in expression during days 3 and 6. NRP1 ligand SEMA3A, which has been described as an inhibitor of neurite outgrowth [32], shows a slight reduction of its expression level in SH-SY5Y^{TNAPlow}, interestingly in an analogous manner compared to NRP1 expression. Expression of SEMA3A however, does not change prominently during treatment in SH-SY5Y^{TNAPhigh} cells (Fig. 3).

Neuronal marker MAP2 shows higher expression in SH-SY5Y^{TNAPhigh} cells on protein level after 3 days of treatment with neurogenic differentiation medium

Staining of SH-SY5Y^{TNAPlow}, SH-SY5Y$^{pcDNA3.1}$ and SH-SY5Y^{TNAPhigh} cells with a specific antibody for the microtubule-binding protein MAP2, which plays an important role e.g. during the outgrowth of neurites [33], reveals the strongest fluorescence signal in the cells with the highest TNAP expression (Fig. 4). Those results after 72 h differentiation are consistent with the qPCR results that indicate a

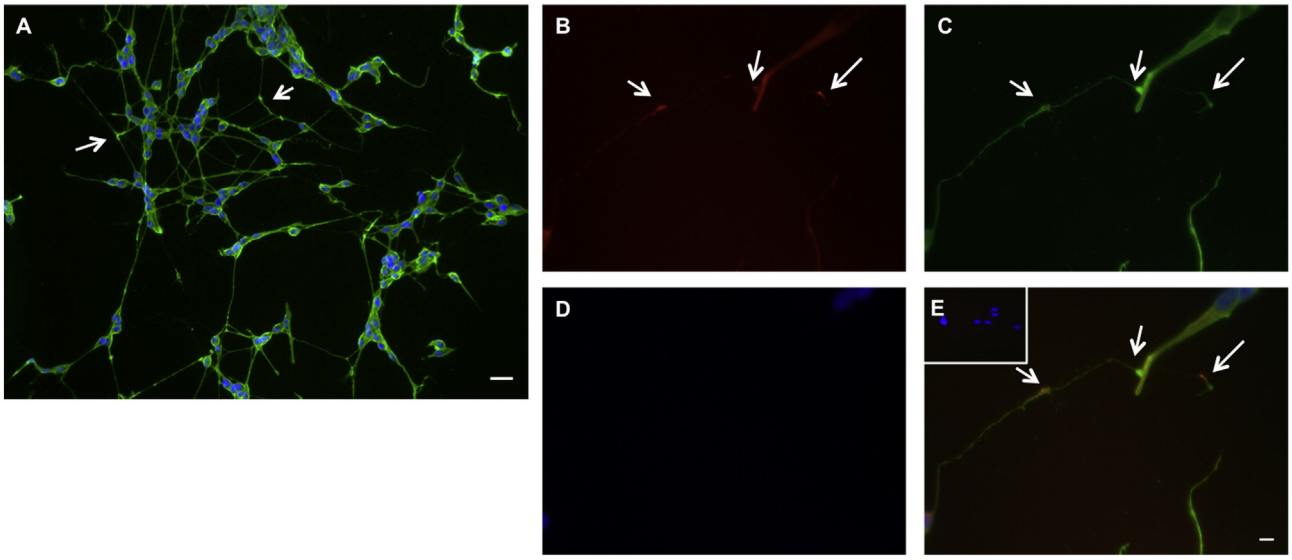

Fig. 2. A. TNAP immunostaining (green) in SH-SY5Y^{TNAPhigh} cells after treatment with differentiation medium for 72 h shows positive staining in the cell membrane including the whole length of the projection network in between the cell bodies. Blue fluorescence represents DAPI-staining of the nucleus. Pictures were taken at 20× magnification and scale bar represents 20 μm. Arrows represent clustered fluorescence signals within the cellular processes. B.–E. Co-localization of synapsin I and TNAP at certain spots in some SH-SY5Y^{TNAPhigh} cells after 72 h of treatment with neurogenic differentiation medium. Pictures were taken at 40× magnification and scale bar represents 10 μm. Arrows represent clustered fluorescence signals. B. Staining of synaptic marker synapsin I in cellular processes (red). C. Staining of TNAP in cellular processes (green). D. DAPI staining of the nuclei (blue). E. Merge of synapsin I (red), TNAP (green) and DAPI (blue) staining in cellular processes. (For interpretation of the references to color in this figure legend, the reader is referred to the web version of this article.)

constantly higher expression of MAP2 in SH-SY5Y^{TNAPhigh} cells until day 6 (Fig. 3). Interestingly, SH-SY5Y^{TNAPlow} cells do not change their MAP2 expression on RNA levels until day 6, but due to a sudden increase, the expression of MAP2 is even higher in those cells after reaching day 10 of treatment. The latter observation might further indicate a retarded differentiation procedure in cells with low TNAP expression.

SH-SY5Y^{TNAPhigh} cells have longer processes after treatment with neurogenic differentiation medium

As GOstat analysis, qPCR results and MAP2 immunostaining provided an indication of TNAP's influence during neurogenic differentiation we further compared the cell lines concerning their morphology. Morphological analysis gives the impression that SH-SY5Y^{TNAPhigh} cells develop longer cellular processes already at an earlier time point of treatment compared to the other two cell lines. SH-SY5Y^{TNAPhigh} cells are able to create a precise network structure of long and quite branched cellular processes (Fig. 5A). None of the three cell lines abandons proliferation completely during treatment with differentiation media.

Projection lengths of individual cell lines were measured on coded pictures with ImageJ 1.49j and mean values of the different approaches were compared to each other. Mean values of all measured processes from three independent experiments are depicted in Fig. 5B, ordered by cell lines and time points. From the very first day of treatment SH-SY5Y^{TNAPhigh} cells show the longest processes. The most obvious discrepancy can be seen after 4 days of treatment with neurogenic differentiation media as SH-SY5Y^{TNAPlow} and SH-SY5Y$^{pcDNA3.1}$ cell lines have a mean projection length of 62.42 and 68.74 μm whereas TNAP overexpressing cells show a mean of 98.88 μm. The total maximum value is reached by SH-SY5Y^{TNAPhigh} at day 6 of the experimental setup. At this time point SH-SY5Y^{TNAPhigh} cells have a mean projection length of 114.29 μm, SH-SY5Y^{TNAPlow} 73.74 μm and SH-SY5Y$^{pcDNA3.1}$ 67.37 μm. SH-SY5Y^{TNAPlow} cells show a 2.5-fold increase of projection length during the whole process, whereas the SH-SY5Y$^{pcDNA3.1}$ cell line does not show any noteworthy increase of length after day 4. In contrast, SH-SY5Y^{TNAPhigh} cells increase their processes' lengths 3.1-fold between t_0 and day 8. For statistical analysis two-way ANOVA and Tukey post-hoc test were calculated. SH-SY5Y$^{pcDNA3.1}$ cells have significantly shorter processes than the other two cell lines (SH-SY5Y^{TNAPlow} $p < 0.001$; SH-SY5Y^{TNAPhigh} $p = 0.011$) at the starting point t_0 and significantly shorter than SH-SY5Y^{TNAPhigh} at day 1 ($p = 0.006$). At days 4 and 6 of neurogenic differentiation the SH-SY5Y^{TNAPhigh} cells have significantly longer processes than SH-SY5Y$^{pcDNA3.1}$ and SH-SY5Y^{TNAPlow} (all p-values < 0.001). At day 8 SH-SY5Y$^{pcDNA3.1}$ cells have significantly shorter processes compared to the other two cell lines (both p-values < 0.001).

Double staining for TNAP and either for tau or MAP2 was performed in SH-SY5Y^{TNAPhigh} cells in order to unravel the nature of the outgrown cellular processes in the course of differentiation. Those experiments reveal an increase of MAP2 and tau signals during differentiation in a subpopulation of the cells, indicating that those cells generate cellular processes which are developing in the direction of either axonal or dendritic structures respectively (Suppl. Figs. 2 and 3). We get the impression that tau protein is located throughout the whole length of the cellular processes until the ramified tips, whereas MAP2 is above all concentrated at the origin of the processes and weakens in the direction of the tips. We were not able to find a clear correlation between TNAP localization and tau or MAP2 staining, since TNAP was actually prevalent in the whole cellular membrane in a very high concentration. Whether the outgrown cellular processes are able to transmit neuronal signals in a proper manner needs to be determined in future experiments.

Discussion

Since data from mouse genetics, clinical CNS-related symptoms of patients suffering from HPP and the physiological expression pattern of TNAP in the human CNS suggest a specific role of tissue-nonspecific alkaline phosphatase in neuronal tissues, we intended to further unravel the molecular mechanisms by creating a transgenic neuroblastoma cell line, which is constantly overexpressing the *ALPL* gene (SH-SY5Y^{TNAPhigh}). We are able to prove the stable integration of the overexpression construct into the genome of SH-SY5Y^{TNAPlow} cells, which have very low endogenous TNAP activity, by analysis of genomic DNA with specific primer combinations. Moreover, semi-quantitative PCRs and Western blot analysis show that the level of TNAP mRNA as well as protein cells is much higher in SH-SY5Y^{TNAPhigh} compared to SH-SY5Y^{TNAPlow} and SH-SY5Y$^{pcDNA3.1}$ cells respectively. Immunocytochemical staining with TNAP-specific antibodies confirms proper localization of the enzyme in the cell membrane as well as a very high TNAP-

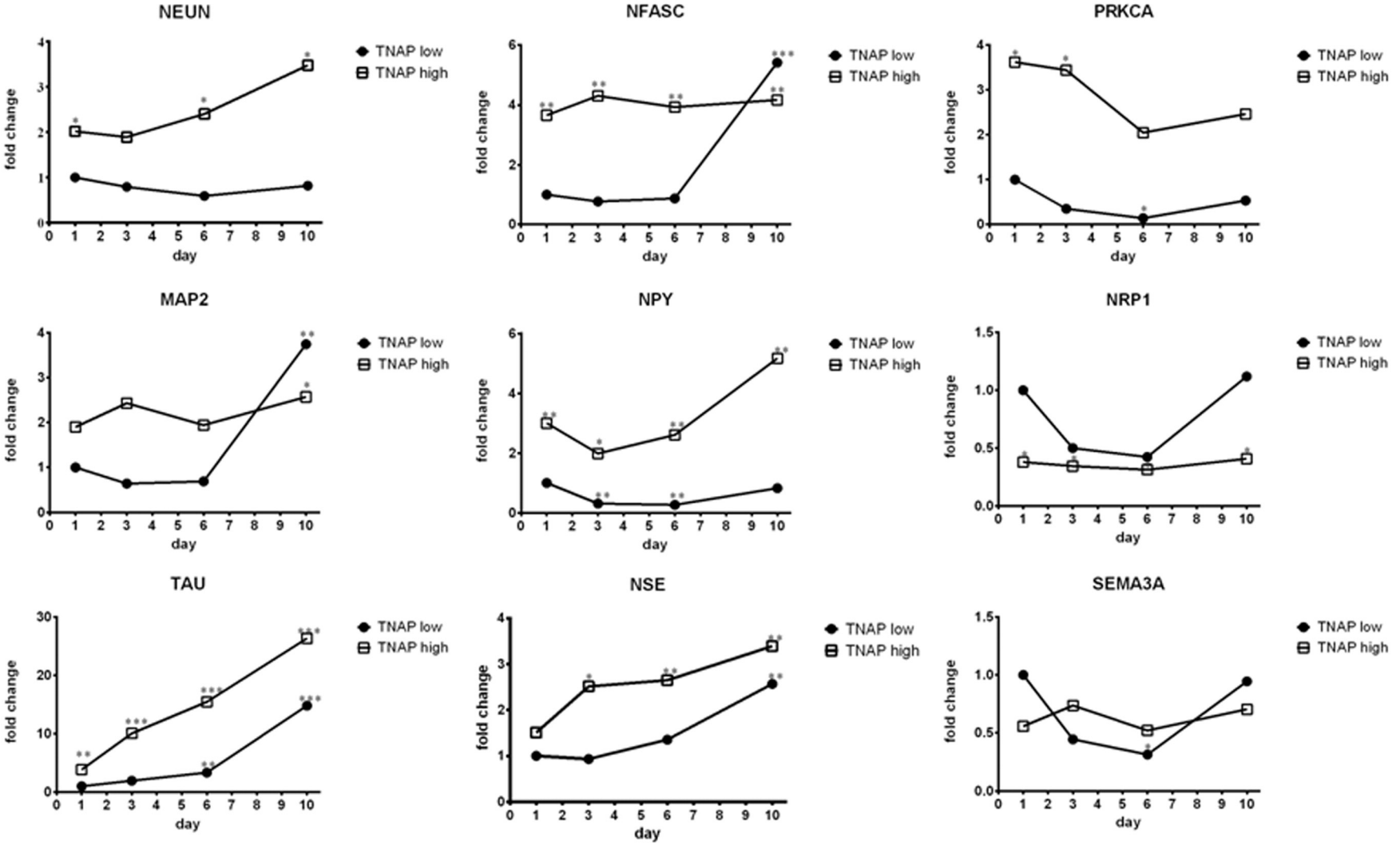

Fig. 3. qPCR results comparing SH-SY5Y^{TNAPhigh} to SH-SY5Y^{TNAPlow} cells after treatment with neurogenic differentiation medium for 1, 3, 6 and 10 days depicted as fold changes in reference to expression values for SH-SY5Y^{TNAPlow} at day 1. RPS27A (ribosomal protein S27a) was used as a housekeeping gene for normalization. Data originate from three independent experiments and PCRs were pipetted three times independently. MAP2 (microtubule-associated protein, 2), NSE (enolase 2, gamma neuronal), SEMA3A (semaphorin 3A), NPY (neuropeptide Y), PRKCA (proteinkinase c, alpha), NFASC (neurofascin), TAU (microtubule-associated protein tau), NRP1 (neuropilin 1) and NEUN (RNA-binding protein, fox-1 homolog 3). Calculations and statistics, both in reference to values for SH-SY5Y^{TNAPlow} at day 1, were done with the software REST 2009 [27]. *$p < 0.05$; **$p < 0.01$; ***$p < 0.001$.

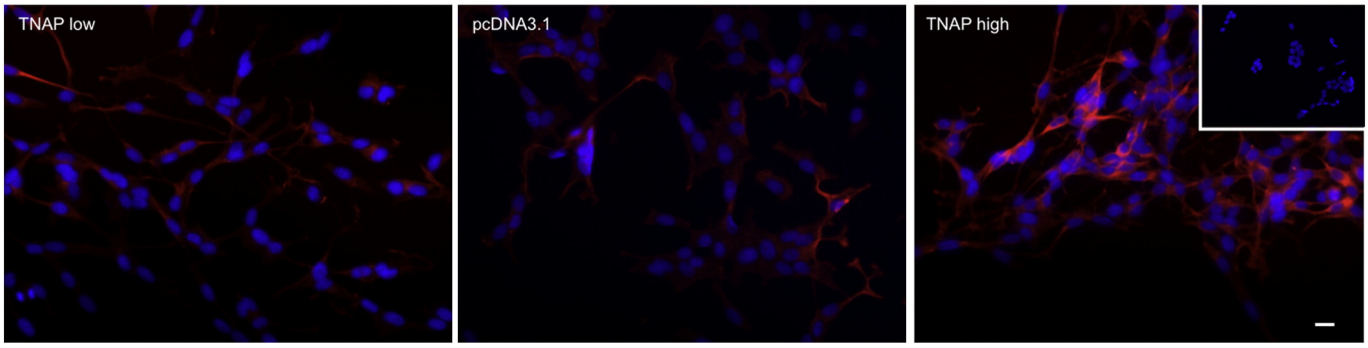

Fig. 4. MAP2 (red) staining of SH-SY5Y^{TNAPlow}, SH-SY5Y$^{pcDNA3.1}$ and SH-SY5Y^{TNAPhigh} cells after 72 h treatment with differentiation medium shows the strongest staining in SH-SY5Y^{TNAPhigh} cells. Blue fluorescence represents DAPI-staining of the nucleus. Reactivity of the secondary antibody with unspecific mouse antigens was excluded since no staining could be seen in samples which were treated with mouse serum instead of the primary antibody (white box). Pictures were taken at 20× magnification and scale bar represents 20 μm. Experiment was repeated four times independently. (For interpretation of the references to color in this figure legend, the reader is referred to the web version of this article.)

expression level in SH-SY5Y^{TNAPhigh}. Enzymatic assays with CSPD reagent as a substrate proof the functionality of the synthesized enzyme and show that the TNAP-specific inhibitor levamisole [34] inhibits enzymatic activity to a great extent (Figs. 1A–D).

After characterization of the established cell lines with different TNAP activity levels, a comparison between those cells was done in order to gain further information about TNAP's role in neuronal surroundings. Nevertheless, one must take into consideration that huge differences in TNAP activity levels might on the one hand intensify effects, but on the other hand one needs to be aware that SH-SY5Y^{TNAPlow} cells might lack some key players, which are relevant in analogous processes in the body since they have such a low endogenous AP. But taking into consideration that experiments with primary cells like murine hippocampal neurons [18] provided similar results gives confidence in our human cell culture model.

Microarray analyses comparing untreated SH-SY5Y^{TNAPlow} and SH-SY5Y^{TNAPhigh} cells (Table 3) as well as differentiated ones (data not shown) reveal an interesting effect of TNAP on processes involved in neurogenesis like projection development which goes along with previous findings published by Diez-Zaera et al. [18]. Comparison of gene expression of SH-SY5Y^{TNAPhigh} and SH-SY5Y^{TNAPlow} cells shows a significant down-regulation of neuropilin 1 and its ligand semaphorin 3A. The latter regulates axon growth cone collapse via Rab5 [35] and can act as an axon repellent as well as an attractant depending on cGMP and cAMP pathways [36]. Moreover, NRP1 and SEMA3A were found to provoke distal axonopathy and muscle denervation in mouse models for amyotrophic lateral sclerosis (ALS) [37]. Differential gene regulation of those two genes proposes an additional mechanism of projection development regulation via TNAP apart from controlling the availability of its substrate ATP which was previously suggested [18]. Another interesting aspect is that semaphorins contribute to growth inhibition of axons in injured neurons of the central nervous system [32], suggesting a possible role of TNAP during regeneration of neurons after injury. Sema3A is further involved in polarization of neurons and regulates branching of dendrites [38,39]. Expression of genes encoding doublecortin, neurexin 1 and protein kinase C α was increased in TNAP overexpressing cells. DCX is a microtubule-associated protein that is involved in migration and differentiation of immature neurons e.g. during development of the cortex [40]. Moreover, a lack of DCX correlates with the appearance of spontaneous epileptic seizures [41] which is indeed very interesting as some severely affected HPP patients also suffer from seizures correlating with the level of available pyridoxal-5′-phosphate in the brain [2]. Langer et al. found that TNAP is located in immature cells of proliferative zones in brains of mouse embryos as well as in the subventricular zone (SVZ) of adults and seems to decrease during progressing neuronal maturation [19]. Nevertheless, a certain population of young neurons of the SVZ shows co-expression of DCX and TNAP [19]. Furthermore, Neurexin 1 is involved in synaptic adhesions and differentiation of neurons [42]. PRKCA was found to be enriched in growth cones of differentiating SH-SY5Y cells, and therefore a role during neurite outgrowth was proposed previously [43]. Additionally, ROBO2 is involved in axonal guidance [44] and NEUN has been described as a specific neuronal protein located in the nucleus [45]. CNTNAP is known for mediating cell-cell interactions in the nervous system and consequently e.g. involved in schizophrenia and major depression [46]. In summary qPCR results further emphasize TNAP's role in neuronal surroundings by suggesting differential expression of genes involved in relevant processes of neurogenesis.

Immunocytochemical stainings of SH-SY5Y^{TNAPhigh} cells after 72 h of neurogenic differentiation reveal localization of TNAP in the cell membrane surrounding the cell bodies as well as throughout the whole length of the cellular processes (Fig. 2A). Prominent fluorescence signals for TNAP were co-localized with synaptic marker synapsin I at some spots (Figs. 2B–E), going along with the findings made in hippocampal neurons which showed strong TNAP staining, above all at terminal ends of the processes [18]. Interestingly, the number of synapsin I positive sites in the established network structure increases considerably after 8 days of neurogenic differentiation. Therefore, we hypothesize that SH-SY5Y^{TNAPhigh} cells develop at least synaptic-like structures, triggered by treatment with differentiation medium. Nonetheless, additional electrophysiological analyses are indispensable in order to gain information about the functionality of those structures. However, we were not able to see a clear correlation between TNAP localization and synapsin I at this time point. Due to their intense and continuous TNAP expression SH-SY5Y^{TNAPhigh} cells probably have limitations for the analysis of fine and distinct subcellular localization and co-localization of TNAP with other subcellular markers. Nonetheless, the lack of glia cells must be considered as another limitation of our model, since astrocytes are known to be involved in processes like maintenance of homoeostasis at synapses as well as regulation the synaptic activity [47].

In order to test whether cells with higher TNAP activity show enhanced differentiation, we compared expression of neuronal markers via qPCR at different time points of treatment with neurogenic differentiation medium. A striking finding was the strong reaction of SH-SY5Y^{TNAPhigh} cells towards stimulation with RA which was leading to a dramatic upregulation of its receptor RARβ. Being less pronounced in SH-SY5Y^{TNAPlow} cells, this effect leads to the assumption that cells with a higher TNAP activity show a higher susceptibility to neurogenic commitment which is finally leading to an acceleration of the differentiation process. The upregulation of TNAP expression in SH-SY5Y^{TNAPlow} cells after treatment with RA (Suppl. Fig. 1) further

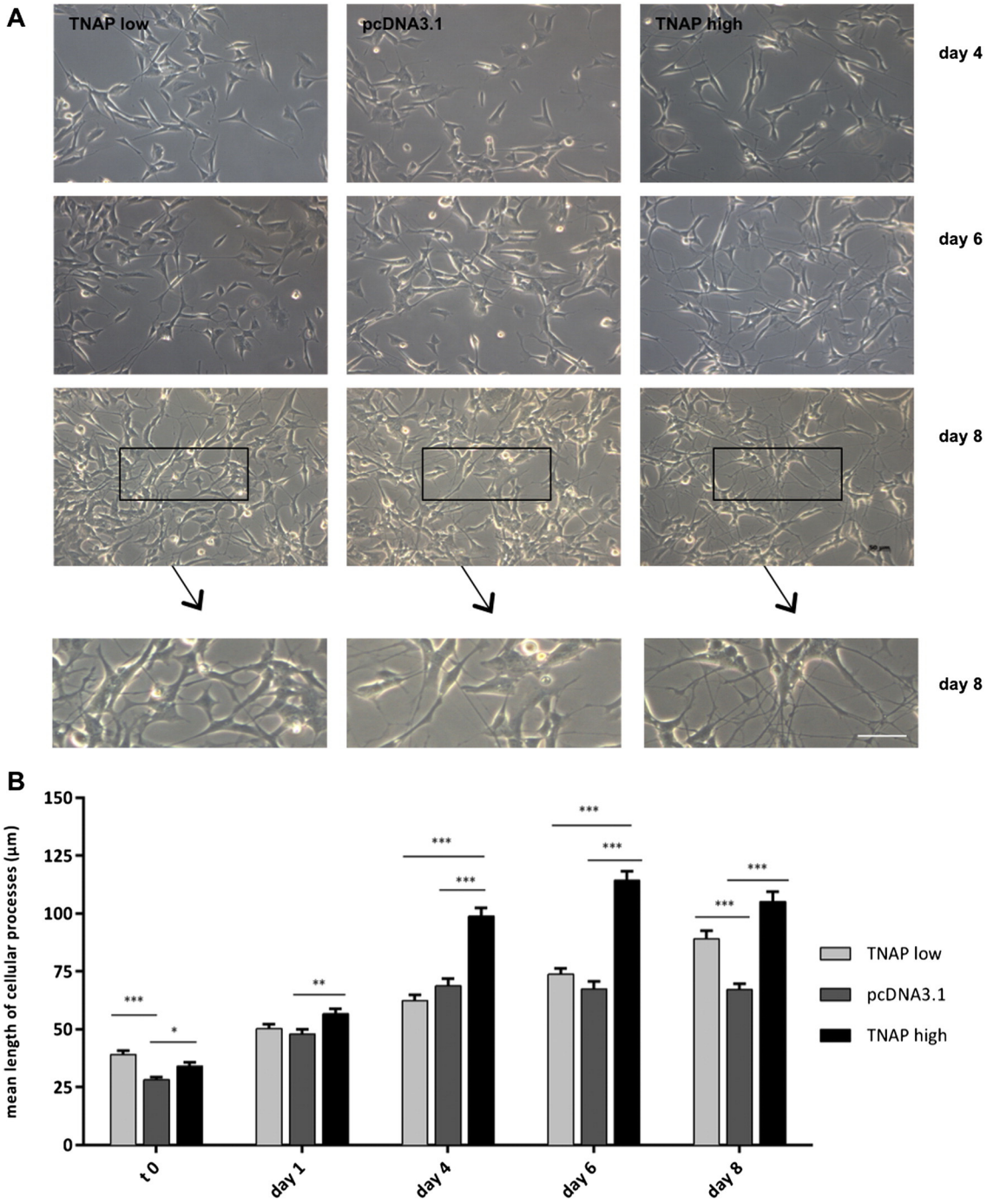

Fig. 5. A. TNAP overexpression influences the outgrowth of cellular processes during neurogenic differentiation. Representative pictures of each cell line at days 4, 6 and 8 have been selected (n = 3). SH-SY5Y^{TNAPlow} and SH-SY5Y$^{pcDNA3.1}$ develop shorter cellular processes compared to the SH-SY5Y^{TNAPhigh} cells. Pictures were taken at 20× magnification and scale bar represents 50 µm. Sections (marked with black boxes) were digitally enlarged for clarification of the differences between the three cell lines. Scale bar represents 50 µm analogously. B. Mean of projection length shows highest values for SH-SY5Y^{TNAPhigh} cells in the course of neurogenic differentiation (days 1–8). Experiments were carried out three times independently. 8 pictures of each cell line were taken randomly at each time point in each experiment. Lengths of 10 processes per photo were measured with the program ImageJ 1.49j after pictures had been coded randomly in a blinded fashion for the operator. Mean values and SEM were calculated from a total of 240 values (at least 140) for a certain cell line at a certain time point. Two-way ANOVA and Tukey post-hoc test were calculated with the program SPSS. *$p < 0.05$; **$p < 0.01$; ***$p < 0.001$.

supports this hypothesis. Going along with our findings, Wan et al. observed an upregulation of TNAP expression by chromatin remodeling at promoter regions of the gene which was triggered by RA [48].

The expression of selected marker genes in the course of neurogenic differentiation (Fig. 3) indicates that SH-SY5Y^{TNAPhigh} cells seem to be somehow ahead of SH-SY5Y^{TNAPlow} cells concerning their differentiation status. Taken together, those data suggest that TNAP activity might be more important at earlier stages of neurogenic differentiation. This goes along with findings made by Langer et al. who proposed a decrease of TNAP activity during maturation of neurons in mouse brains [19]. NEUN is a widely-used neuronal marker as it is solely expressed in neurons, more specifically located in their nuclei, and might be responsible for neuron specific splicing processes [45]. NPY regulates synaptic transmission and is furthermore involved in anxiety disorders which can also be seen in HPP patients [49,50]. Moreover higher expression levels of NSE and NFASC in SH-SY5Y^{TNAPhigh} cells gives further proof

of enhanced differentiation into a neuronal phenotype. Interestingly, neurofascin is important for the establishment of saltatory conduction along myelinated axons [51] and speculations about a contribution of TNAP to the process of myelination have been published as well [15]. Surprisingly, SH-SY5Y^{TNAPlow} cells show a clear increase of NFASC expression at the late time points, which might indicate that those cells gradually catch up with the TNAP over expressing cell line over time.

Above all the microtubule-binding protein tau is constantly expressed on a higher level in SH-SY5Y^{TNAPhigh} than in SH-SY5Y^{TNAPlow} cells and a clear increase in expression is obvious on RNA and protein levels (Fig. 3, Suppl. Fig. 2) in both cell lines in the course of the differentiation process. Tau plays a role in polarization of neurites [52] and is translocated from the nucleus to cytosol during the differentiation process [53]. Additionally, we observed higher MAP2 protein expression in SH-SY5Y^{TNAPhigh} cells compared to the other two cell lines (Fig. 4) as well as an increased expression of MAP2 on the protein level in the course of neurogenic differentiation in some cells (Suppl. Fig. 3). Microtubule-binding proteins like MAP2 and tau play a central role in stabilizing microtubules, consequently providing axonal transport [54]. MAP2 and tau seem to have complementary functions during the outgrowth of neurites, since MAP2 is above all necessary for the initiation and tau for the elongation of the cellular processes [33]. Moreover, MAP2 is mainly concentrated in dendrites [55], whereas tau protein is usually localized in the axon and was also found to be associated with the membranes of Golgi apparatus [56]. However, high expression of tau is also involved in pathological neuronal cell death like it has been described in prion disease as increased total tau protein and hyperphosphorylation of tau are associated with terminal stages of this disease [29,54]. There is also a connection between TNAP and Alzheimer's disease (AD) as serum and brain levels of TNAP correlate with severity of AD. Progression of the disease and subsequent neurodegeneration can be further promoted by TNAP as the enzyme dephosphorylates extracellular tau which afterwards activates muscarinergic receptors and finally causes neuronal death [57,58]. Taken together, we see a clear indication of a necessity for TNAP during neuronal development and neurogenic differentiation which is going along with previously published clinical findings [2] and triggered via stimulation of relevant proteins. In contrast, high levels of TNAP enzyme may propagate certain neurodegenerative conditions in pathology.

A participation of TNAP in the process of neurogenesis and projection development could further be confirmed by the observation of morphological differences between the cell lines during treatment with neurogenic differentiation media based on RA. Cells with higher TNAP levels have longer cellular processes and develop networks that are more distinct than the other two cell lines, without clear differences in cell numbers or proportion of processes per cell in between the three examined cell lines. The reason why values did not constantly increase might be due to the higher cell density, which causes a lack of space between cell bodies after 6–8 days. Another possibility might be that measurements in samples with higher cell density can probably not be considered as reliable as in the ones with lower cell density since parts of the processes might be covered by cell bodies of neighboring cells and consequently underestimated. It is striking that above all SH-SY5Y$^{pcDNA3.1}$ cells stop the continuous elongation of their cellular processes. We cannot exclude that the integration of the pcDNA3.1 vector caused this effect since the exact position of integration into the genome is unknown. However, this observation even intensifies the effect caused by TNAP since SH-SY5Y^{TNAPhigh} cells were also stably transfected and therefore underwent the analogous procedure as SH-SY5Y$^{pcDNA3.1}$ cells.

Conclusion

The results indicate that TNAP is far more than an indispensable enzyme for bone metabolism. We could confirm an influence of TNAP on processes which are important for proper development of the nervous system in our *in vitro* model. TNAP expression has a clear impact on neuronal systems as it influences outgrowth of cellular processes and induces higher expression of genes which are playing important roles during myelination, synaptic transmission and neurite outgrowth (like NEUN, NSE, MAP2 and TAU). It will be of further interest whether the results gained from the neuroblastoma cell lines can be confirmed in primary neural stem cells prepared from our previously published mouse models for hypophosphatasia [59]. In humans TNAP activity can be assigned to distinct cortical regions, corresponding to layers 4 and 5, where integration of information from various brain regions takes place [12,13,60]. TNAP might therefore play a role in the fine tuning of the information exchange. Moreover, high TNAP activity may also be involved in the pathology of neurodegenerative diseases and in atherosclerosis, both very common age-related diseases [29,57,61,62]. Unraveling the molecular role of TNAP in systems inside and outside the bone will help to improve treatment strategies for HPP patients. Taking this rare disease as a model will also help to dissect TNAP's role in degenerative diseases and might enable future treatment of those common pathologies by targeting this enzyme.

Supplementary data to this article can be found online at http://dx.doi.org/10.1016/j.bone.2015.05.033.

Funding

This work was funded by HPP patients' organization Hypophosphatasie Deutschland e.V. and Elsbeth Bonhoff Foundation (Zuwendungsgesuch 109) (Berlin, Germany).

Conflict of interest statement

None to declare.

Acknowledgments

We thank Prof. Klaus-Peter Lesch for providing the SH-SY5Y neuroblastoma cell line and Prof. Anna-Leena Sirén, Barbara Gado, Dr. Regina Ebert and Juliane Pochhammer for their helpful support.

References

[1] Whyte MP. Physiological role of alkaline phosphatase explored in hypophosphatasia. Ann N Y Acad Sci 2010;1192:190–200.
[2] Hofmann C, et al. Compound heterozygosity of two functional null mutations in the ALPL gene associated with deleterious neurological outcome in an infant with hypophosphatasia. Bone 2013;55(1):150–7.
[3] Moss DW, et al. Association of inorganic-pyrophosphatase activity with human alkaline-phosphatase preparations. Biochem J 1967;102(1):53–7.
[4] Narisawa S, Yadav MC, Millan JL. In vivo overexpression of tissue-nonspecific alkaline phosphatase increases skeletal mineralization and affects the phosphorylation status of osteopontin. J Bone Miner Res 2013;28(7):1587–98.
[5] Harmey D, et al. Concerted regulation of inorganic pyrophosphate and osteopontin by akp2, enpp1, and ank: an integrated model of the pathogenesis of mineralization disorders. Am J Pathol 2004;164(4):1199–209.
[6] Yadav MC, et al. Ablation of osteopontin improves the skeletal phenotype of phospho1(−/−) mice. J Bone Miner Res 2014;29(11):2369–81.
[7] Yadav MC, et al. Loss of skeletal mineralization by the simultaneous ablation of PHOSPHO1 and alkaline phosphatase function: a unified model of the mechanisms of initiation of skeletal calcification. J Bone Miner Res 2011;26(2):286–97.
[8] Nayudu RV, de Meis L. Energy transduction at the catalytic site of enzymes: hydrolysis of phosphoester bonds and synthesis of pyrophosphate by alkaline phosphatase. FEBS Lett 1989;255(1):163–6.
[9] Ohkubo S, Kimura J, Matsuoka I. Ecto-alkaline phosphatase in NG108-15 cells: a key enzyme mediating P1 antagonist-sensitive ATP response. Br J Pharmacol 2000;131(8):1667–72.
[10] Zimmermann H, Zebisch M, Strater N. Cellular function and molecular structure of ecto-nucleotidases. Purinergic Signal 2012;8(3):437–502.
[11] Brun-Heath I, et al. Differential expression of the bone and the liver tissue non-specific alkaline phosphatase isoforms in brain tissues. Cell Tissue Res 2011;343(3):521–36.
[12] Negyessy L, et al. Layer-specific activity of tissue non-specific alkaline phosphatase in the human neocortex. Neuroscience 2011;172:406–18.
[13] Fonta C, et al. Areal and subcellular localization of the ubiquitous alkaline phosphatase in the primate cerebral cortex: evidence for a role in neurotransmission. Cereb Cortex 2004;14(6):595–609.

[14] Fonta C, et al. Postnatal development of alkaline phosphatase activity correlates with the maturation of neurotransmission in the cerebral cortex. J Comp Neurol 2005; 486(2):179–96.
[15] Hanics J, et al. Ablation of TNAP function compromises myelination and synaptogenesis in the mouse brain. Cell Tissue Res 2012;349(2):459–71.
[16] Kermer V, et al. Knockdown of tissue nonspecific alkaline phosphatase impairs neural stem cell proliferation and differentiation. Neurosci Lett 2010;485(3):208–11.
[17] Narisawa S, et al. Stage-specific expression of alkaline phosphatase during neural development in the mouse. Dev Dyn 1994;201(3):227–35.
[18] Diez-Zaera M, et al. Tissue-nonspecific alkaline phosphatase promotes axonal growth of hippocampal neurons. Mol Biol Cell 2011;22(7):1014–24.
[19] Langer D, et al. The ectonucleotidases alkaline phosphatase and nucleoside triphosphate diphosphohydrolase 2 are associated with subsets of progenitor cell populations in the mouse embryonic, postnatal and adult neurogenic zones. Neuroscience 2007;150(4):863–79.
[20] Manegold C, et al. Aromatic L-amino acid decarboxylase deficiency: clinical features, drug therapy and follow-up. J Inherit Metab Dis 2009;32(3):371–80.
[21] Clayton PT. B6-responsive disorders: a model of vitamin dependency. J Inherit Metab Dis 2006;29(2–3):317–26.
[22] Balasubramaniam S, et al. Perinatal hypophosphatasia presenting as neonatal epileptic encephalopathy with abnormal neurotransmitter metabolism secondary to reduced co-factor pyridoxal-5′-phosphate availability. J Inherit Metab Dis 2010; 33(Suppl. 3):S25–33.
[23] Kantor O, et al. TNAP activity is localized at critical sites of retinal neurotransmission across various vertebrate species. Cell Tissue Res 2014;358(1):85–98.
[24] Langer D, et al. Distribution of ectonucleotidases in the rodent brain revisited. Cell Tissue Res 2008;334(2):199–217.
[25] Mentrup B, et al. Functional characterization of a novel mutation localized in the start codon of the tissue-nonspecific alkaline phosphatase gene. Bone 2011;48(6): 1401–8.
[26] Lee JH, et al. Neurogenic differentiation of human dental stem cells in vitro. J Korean Assoc Oral Maxillofac Surg 2014;40(4):173–80.
[27] Pfaffl MW, Horgan GW, Dempfle L. Relative expression software tool (REST) for group-wise comparison and statistical analysis of relative expression results in real-time PCR. Nucleic Acids Res 2002;30(9):e36.
[28] El Andaloussi-Lilja J, Lundqvist J, Forsby A. TRPV1 expression and activity during retinoic acid-induced neuronal differentiation. Neurochem Int 2009;55(8):768–74.
[29] Ermonval M, et al. The cellular prion protein interacts with the tissue non-specific alkaline phosphatase in membrane microdomains of bioaminergic neuronal cells. PLoS One 2009;4(8):e6497.
[30] Beissbarth T, Speed TP. GOstat: find statistically overrepresented Gene Ontologies within a group of genes. Bioinformatics 2004;20(9):1464–5.
[31] de The H, et al. Differential expression and ligand regulation of the retinoic acid receptor alpha and beta genes. EMBO J 1989;8(2):429–33.
[32] Pasterkamp RJ, Verhaagen J. Semaphorins in axon regeneration: developmental guidance molecules gone wrong? Philos Trans R Soc Lond B Biol Sci 2006;361(1473): 1499–511.
[33] Caceres A, Mautino J, Kosik KS. Suppression of MAP2 in cultured cerebellar macroneurons inhibits minor neurite formation. Neuron 1992;9(4):607–18.
[34] Van Belle H. *Alkaline phosphatase.* I. Kinetics and inhibition by levamisole of purified isoenzymes from humans. Clin Chem 1976;22(7):972–6.
[35] Song H, et al. Conversion of neuronal growth cone responses from repulsion to attraction by cyclic nucleotides. Science 1998;281(5382):1515–8.
[36] Wu KY, et al. Semaphorin 3A activates the guanosine triphosphatase Rab5 to promote growth cone collapse and organize callosal axon projections. Sci Signal 2014; 7(340):ra81.
[37] Venkova K, et al. Semaphorin 3A signaling through neuropilin-1 is an early trigger for distal axonopathy in the SOD1G93A mouse model of amyotrophic lateral sclerosis. J Neuropathol Exp Neurol 2014;73(7):702–13.
[38] Arikkath J. Molecular mechanisms of dendrite morphogenesis. Front Cell Neurosci 2012;6:61.
[39] Shelly M, et al. Semaphorin3A regulates neuronal polarization by suppressing axon formation and promoting dendrite growth. Neuron 2011;71(3):433–46.
[40] Francis F, et al. Doublecortin is a developmentally regulated, microtubule-associated protein expressed in migrating and differentiating neurons. Neuron 1999;23(2): 247–56.
[41] Kerjan G, et al. Mice lacking doublecortin and doublecortin-like kinase 2 display altered hippocampal neuronal maturation and spontaneous seizures. Proc Natl Acad Sci U S A 2009;106(16):6766–71.
[42] Zeng L, et al. Functional impacts of NRXN1 knockdown on neurodevelopment in stem cell models. PLoS One 2013;8(3):e59685.
[43] Parrow V, et al. Protein kinase C-alpha and -epsilon are enriched in growth cones of differentiating SH-SY5Y human neuroblastoma cells. J Neurosci Res 1995;41(6): 782–91.
[44] Jaworski A, Long H, Tessier-Lavigne M. Collaborative and specialized functions of Robo1 and Robo2 in spinal commissural axon guidance. J Neurosci 2010;30(28): 9445–53.
[45] Kim KK, Adelstein RS, Kawamoto S. Identification of neuronal nuclei (NeuN) as Fox-3, a new member of the Fox-1 gene family of splicing factors. J Biol Chem 2009;284(45):31052–61.
[46] Ji W, et al. CNTNAP2 is significantly associated with schizophrenia and major depression in the Han Chinese population. Psychiatry Res 2013;207(3):225–8.
[47] Perea G, Sur M, Araque A. Neuron-glia networks: integral gear of brain function. Front Cell Neurosci 2014;8:378.
[48] Wan Y, et al. All-trans retinoic acid induces chromatin remodeling at the promoter of the mouse liver, bone, and kidney alkaline phosphatase gene in C3H10T 1/2 cells. Biochem Genet 2012;50(7–8):495–507.
[49] Donner J, et al. Support for involvement of glutamate decarboxylase 1 and neuropeptide Y in anxiety susceptibility. Am J Med Genet B Neuropsychiatr Genet 2012; 159B(3):316–27.
[50] Bacci A, Huguenard JR, Prince DA. Differential modulation of synaptic transmission by neuropeptide Y in rat neocortical neurons. Proc Natl Acad Sci U S A 2002; 99(26):17125–30.
[51] Sherman DL, et al. Neurofascins are required to establish axonal domains for saltatory conduction. Neuron 2005;48(5):737–42.
[52] Caceres A, Kosik KS. Inhibition of neurite polarity by tau antisense oligonucleotides in primary cerebellar neurons. Nature 1990;343(6257):461–3.
[53] Uberti D, et al. Characterization of tau proteins in human neuroblastoma SH-SY5Y cell line. Neurosci Lett 1997;235(3):149–53.
[54] Zhang J, Dong XP. Dysfunction of microtubule-associated proteins of MAP2/tau family in Prion disease. Prion 2012;6(4):334–8.
[55] Huber G, Matus A. Differences in the cellular distributions of two microtubule-associated proteins, MAP1 and MAP2, in rat brain. J Neurosci 1984;4(1):151–60.
[56] Farah CA, et al. Tau interacts with Golgi membranes and mediates their association with microtubules. Cell Motil Cytoskeleton 2006;63(11):710–24.
[57] Diaz-Hernandez M, et al. Tissue-nonspecific alkaline phosphatase promotes the neurotoxicity effect of extracellular tau. J Biol Chem 2010;285(42):32539–48.
[58] Gomez-Ramos A, et al. Extracellular tau promotes intracellular calcium increase through M1 and M3 muscarinic receptors in neuronal cells. Mol Cell Neurosci 2008;37(4):673–81.
[59] Mentrup B, et al. In vitro characterization of TNSALP mutations from two novel mouse models for hypophosphatasia. Bull Group Int Rech Sci Stomatol Odontol 2012;51(1):e33.
[60] Hill DN, et al. Multibranch activity in basal and tuft dendrites during firing of layer 5 cortical neurons in vivo. Proc Natl Acad Sci U S A 2013;110(33):13618–23.
[61] Vardy ER, et al. Alkaline phosphatase is increased in both brain and plasma in Alzheimer's disease. Neurodegener Dis 2012;9(1):31–7.
[62] Schoppet M, Shanahan CM. Role for alkaline phosphatase as an inducer of vascular calcification in renal failure? Kidney Int 2008;73(9):989–91.